

The HARPS search for southern extra-solar planets[★]

X. A $m \sin i = 11 M_{\oplus}$ planet around the nearby spotted M dwarf GJ 674

X. Bonfils¹, M. Mayor², X. Delfosse³, T. Forveille³, M. Gillon², C. Perrier³, S. Udry², F. Bouchy⁴, C. Lovis², F. Pepe²,
D. Queloz², N. C. Santos^{1,2,5}, and J.-L. Bertaux⁶

¹ Centro de Astronomia e Astrofísica da Universidade de Lisboa, Observatório Astronómico de Lisboa, Tapada da Ajuda, 1349-018 Lisboa, Portugal e-mail: xavier.bonfils@oal.ul.pt

² Observatoire de Genève, 51 ch. des Maillettes, CH-1290 Sauverny, Switzerland

³ Laboratoire d'Astrophysique, Observatoire de Grenoble, BP 53, F-38041 Grenoble, Cedex 9, France

⁴ Institut d'Astrophysique de Paris, CNRS, Université Pierre et Marie Curie, 98bis Bd Arago, 75014 Paris, France

⁵ Centro de Geofísica de Évora, Rua Romão Ramalho 59, 7002-554 Évora, Portugal

⁶ Service d'Aéronomie du CNRS, BP 3, 91371 Verrières-le-Buisson, France

Received January 09, 2007; accepted xxxx xx, 2007

ABSTRACT

Context. How planet properties depend on stellar mass is a key diagnostic of planetary formation mechanisms.

Aims. This motivates planet searches around stars which are significantly more massive or less massive than the Sun, and in particular our radial velocity search for planets around very-low mass stars.

Methods. As part of that program, we obtained measurements of GJ 674, an M2.5 dwarf at $d=4.5$ pc, which have a dispersion much in excess of their internal errors. An intensive observing campaign demonstrates that the excess dispersion is due to two superimposed coherent signals, with periods of 4.69 and 35 days.

Results. These data are well described by a 2-planet Keplerian model where each planet has a $\sim 11 M_{\oplus}$ minimum mass. A careful analysis of the (low level) magnetic activity of GJ 674 however demonstrates that the 35-day period coincides with the stellar rotation period. This signal therefore originates in a spot inhomogeneity modulated by stellar rotation. The 4.69-day signal on the other hand is caused by a bona-fide planet, GJ 674b.

Conclusions. Its detection adds to the growing number of Neptune-mass planets around M-dwarfs, and reinforces the emerging conclusion that this mass domain is much more populated than the jovian mass range. We discuss the metallicity distributions of M dwarf *with* and *without* planets and find a low 11% probability that they are drawn from the same parent distribution. Moreover, we find tentative evidence that the host star metallicity correlates with the total mass of their planetary system.

Key words. stars: individual: GJ 674 – stars: planetary systems – stars: late-type – technique: radial-velocity

1. Introduction

M dwarfs, the most common stars in our Galaxy, were added to the target lists of planet-search programs soon after the first exoplanet discoveries. Compared to Sun-like stars, they suffer from some drawbacks: they are faint and photon noise therefore often limits measurements of their radial velocity, and many are at least moderately active and thus prone to so-called “radial-velocity jitter” (Saar & Donahue 1997). On the other hand, the smaller masses of M dwarfs result in a higher wobble amplitude for a given planetary mass, and their p-mode oscillations have both smaller amplitudes and shorter periods than those of solar type stars. These oscillations therefore average out much faster. As a result, the detection of an Earth-like planet in the – closer – habitable zone of an M dwarf is actually within reach of today’s best spectrographs. Perhaps most importantly, however, M dwarfs represent unique targets to probe the dependence on stellar mass of planetary formation, thanks to the wide mass range (0.1 to $0.6 M_{\odot}$) spanned by that spectral class alone.

Send offprint requests to: X. Bonfils

[★] Based on observations made with the HARPS instrument on the ESO 3.6 m telescope under the GTO program ID 072.C-0488 at Cerro La Silla (Chile).

The first planet found to orbit an M dwarf, GJ 876b (Delfosse et al. 1998; Marcy et al. 1998), was only the 9th exoplanet discovered around a main sequence star. Besides showing that Jupiter-mass planets can form at all around very-low-mass stars, its discovery suggested that they might be common, since it was found amongst the few dozen M dwarfs that were observed at that time. Against these early expectations, no other M dwarf was reported to host a planet until 2004, though a second planet (GJ 876c, $m_p \sin i = 0.56 M_{\text{Jup}}$ – Marcy et al. 2001) was soon found around GJ 876 itself.

In 2004, the continuous improvement of the radial-velocity techniques resulted in the quasi-simultaneous discovery of three Neptune-mass planets, around μ Ara ($m_p \sin i = 14 M_{\oplus}$ – Santos et al. 2004), ρ Cnc ($m_p \sin i = 14 M_{\oplus}$ – McArthur et al. 2004) and GJ 436 ($m_p \sin i = 23 M_{\oplus}$ – Butler et al. 2004; Maness et al. 2006). Of those three, GJ 436b, orbits an M dwarf, and put that spectral class back on the discovery forefront. It was soon followed by another two, a single planet around GJ 581 ($m_p \sin i = 17 M_{\oplus}$ – Bonfils et al. 2005b) and a very light ($m_p = 7.5 M_{\oplus}$) third planet in the GJ 876 system (Rivera et al. 2005). As a result, planets around M dwarfs today represent a substantial fraction (30%) of all known planets with $m \sin i \lesssim 30 M_{\oplus}$.

Even with GJ 849b ($m_p \sin i = 0.82 M_{\text{Jup}}$ – Butler et al. 2006) now completing the inventory of M-dwarf planets found with radial-velocity techniques, the upper-range of planet masses remains scarcely populated. This contrasts both with the (still very incompletely known) Neptune-mass planets orbiting M dwarfs and with the jovian planets around Sun-like stars. At larger separations, microlensing surveys similarly probe the frequency of planets as a function of their mass. That technique has detected four putative planets that likely orbit M dwarfs: OGLE235-MOA53b ($m_p \sim 1.5 - 2.5 M_{\text{Jup}}$ – Bond et al. 2004), OGLE-05-071Lb ($m_p = 0.9 M_{\text{Jup}}$ – Udalski et al. 2005), OGLE-05-390Lb ($m_p = 0.017 M_{\text{Jup}}$ – Beaulieu et al. 2006) and OGLE-05-169Lb ($m_p = 0.04 M_{\text{Jup}}$ – Gould et al. 2006). Two of these four planets have likely masses below $0.1 M_{\text{Jup}}$. Given the detection bias of that technique towards massive companions, this again suggests that Neptune-mass planets are much more common than Jupiter-mass ones around very-low-mass stars.

Here we report the discovery of a 11 M_{\oplus} planet orbiting GJ 674 every 4.69 days. GJ 674b has the 5th lowest mass of the known planets, and coincidentally is also the 5th planetary system centered on a M dwarf. Its detection adds to the small inventory of both very-low mass planets and planets around very-low mass stars. After reviewing the properties of the GJ 674 star (§2), we briefly present our radial velocity measurements (§3) and their Keplerian analysis (§4). A careful analysis of the magnetic activity of GJ 674 (§5) assigns one of the two periodicities to rotational modulation of a stellar spot signal, and the other one to a *bona fide* planet. We conclude with a brief discussion of the properties of the detected planet.

2. The properties of GJ 674

GJ 674 (HIP 85523, LHS 449) is a M2.5 dwarf (Hawley et al. 1997) in the Altar constellation. At 4.5 pc ($\pi = 220.43 \pm 1.63$ mas – ESA 1997), it is the 37th closest stellar system, the 54th closest star (taking stellar multiplicity into account)¹, and only the 2nd closest known planetary system (after ϵ Eridani, and slightly closer than GJ 876).

Its photometry ($V = 9.382 \pm 0.012$; $K = 4.855 \pm 0.018$ – Turon et al. 1993; Cutri et al. 2003) and parallax imply absolute magnitudes of $M_V = 11.09 \pm 0.04$ and $M_K = 6.57 \pm 0.04$. GJ 674's $J - K$ color ($= 0.86$ – Cutri et al. 2003) and the Leggett et al. (2001) colour-bolometric relation result in a K-band bolometric correction of $BC_K = 2.67$, and in a $0.016 L_{\odot}$ luminosity.

The K-band mass-luminosity relation of Delfosse et al. (2000) gives a $0.35 M_{\odot}$ mass and the Bonfils et al. (2005a) photometric calibration of the metallicity results in $[Fe/H] = -0.28 \pm 0.2$.

The moderate X-ray luminosity ($L_x/L_{bol} \simeq 5.10^{-5}$ – Hünsch et al. 1999) and Ca II H & K emission depict a modestly active M dwarf (Fig. 1). Its UVW galactic velocities place GJ 674 between the young and old disk populations (Leggett 1992), suggesting an age of $\sim 10^{8-9}$ yr.

Last but not least, since we are concerned with radial velocities, the high proper motion of GJ 674 ($1.05 \text{ arcsec yr}^{-1}$ – ESA 1997) changes the orientation of its velocity vector along the line-of-sight (e.g. Kürster et al. 2003) to result in an apparent secular acceleration of $0.115 \text{ m s}^{-1} \text{ yr}^{-1}$. At our current precision this acceleration will not be detectable before another decade.

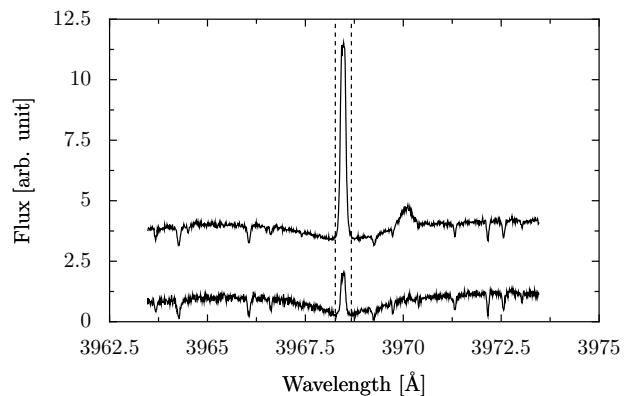


Fig. 1. Emission reversal in the Ca II H line of GJ 674 (top) and GJ 581 (bottom). Within our sample GJ 581 has one of the weakest Ca II emission and illustrates a very quiet M dwarf. GJ 674 has much stronger emission and is moderately active.

Table 1. Observed and inferred stellar parameters for GJ 674

Parameter	GJ 674
Spectral Type	M2.5
V	9.382 ± 0.012
π [mas]	220.43 ± 1.63
Distance [pc]	4.54 ± 0.03
M_V	11.09 ± 0.04
K	4.855 ± 0.018
M_K	6.57 ± 0.04
L_{\star} [L_{\odot}]	0.016
L_x/L_{bol}	5.10^{-5}
$v \sin i$ [km s^{-1}]	$\lesssim 1$
dv_r/dt [$\text{m s}^{-1} \text{ yr}^{-1}$]	0.115
$[Fe/H]$	-0.28
M_{\star} [M_{\odot}]	0.35
age [Gyr]	0.1-1
T_{eff} [K]	3500-3700

3. Radial-velocity data

We observed GJ 674 with the HARPS echelle spectrograph (Mayor et al. 2003) mounted on the ESO 3.6-m telescope at La Silla Observatory (Chile). After demonstrating impressive planet finding capabilities right after its commissioning (Pepe et al. 2004), this spectrograph now defines the state of the art in radial-velocity measurements, delivering a significantly better precision than its ambitious 1 m s^{-1} specification. As one recent published example, Lovis et al. (2006a) obtained a 0.64 m s^{-1} dispersion for the residuals of their orbital solution of the 3 Neptune-mass planets of HD 69830.

We observed GJ 674 without interlaced Thorium-Argon light to obtain cleaner spectra for spectroscopic analysis, at some small cost in the ultimate Doppler precision. Since June 2004 we have gathered 32 exposures of 900 s each with a median S/N ratio of ~ 90 . Their Doppler information content, evaluated according to the prescriptions of Bouchy et al. (2001), is mostly below 1 m s^{-1} . Our internal errors additionally include, in quadrature sum, an “instrumental” uncertainty of 0.5 m s^{-1} for the nightly drift of the spectrograph (since we do not use the ThAr lamp to monitor it) and the measurements uncertainty of the daily wavelength zero point calibration. We did benefit of the recent improvements of the HARPS wavelength calibration, which is now stable to 0.1 m s^{-1} (Lovis et al. 2006b).

A constant radial velocity gives a very large reduced chi-square ($\bar{\chi}^2 = 132$) for the time series, which reflects a disper-

¹ on Mar. 1st 2007 (<http://www.chara.gsu.edu/RECONS/TOP100.htm>)

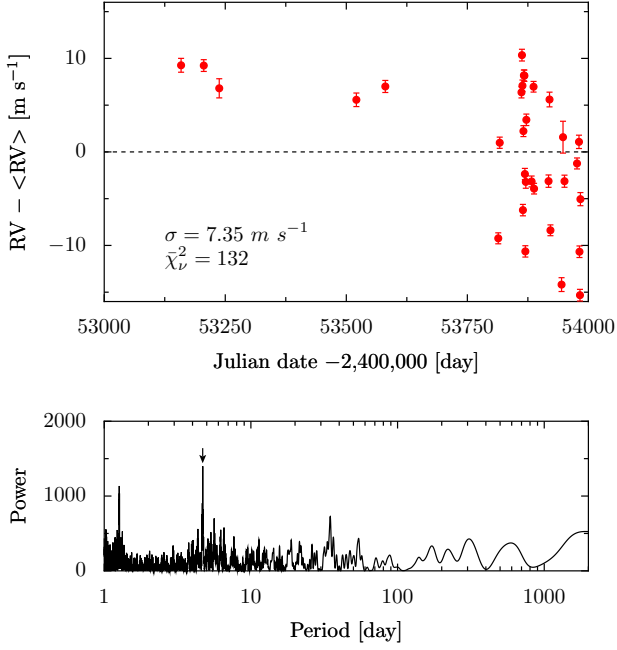


Fig. 2. *Upper panel:* Radial-velocity measurements of GJ 674 as a function of time. The high dispersion ($\sigma = 7.35 \text{ m s}^{-1}$) and chi-square value ($\bar{\chi}^2 = 132$) betray a (coherent or incoherent) signal in the data. *Bottom panel:* the Lomb-Scargle periodogram of the velocities has prominent power excess around $P = 4.69$ days (downward arrow), which indicates that much of the excess dispersion reflects a coherent signal with a period close to that value. The second highest peak, at 1.27 day, is a one-day alias of the 4.69 days period ($1.27 \approx 1 + 1/4.69$).

sion ($\sim 7.4 \text{ m s}^{-1}$) well above our internal errors (Fig. 2). This prompted a search for an orbital (§4) and/or magnetic activity (§5) signal.

4. Orbital analysis

A Lomb-Scargle periodogram (Press et al. 1992) of the velocity measurements shows a narrow peak around 4.69-day (Fig. 2). Adjustment of a single Keplerian orbit demonstrates that it is best described by a $m_2 \sin i = 12.7 M_{\oplus}$ planet ($0.040 M_{\text{Jup}}$) revolving around GJ 674 every $P_2 = 4.6940 \pm 0.0005$ days in a slightly eccentric orbit ($e_2 = 0.10 \pm 0.02$). The residuals around this low-amplitude orbit ($K_1 = 9.8 \pm 0.2 \text{ m s}^{-1}$) have a dispersion of 3.27 m s^{-1} (Fig. 3), still well above our measurement errors, and the reduced chi-square per degree of freedom is $\bar{\chi}^2 = 30.6$. A periodogram of the residuals indicates that much of this excess dispersion stems from a broad power peak centered around 35 days, prompting us to perform a 2-planet fit.

We searched for 2-planet Keplerian solutions with *Stakanof* (Tamuz, in prep.), a program which uses genetic algorithms to efficiently explore the large parameter space of multi-planet models. *Stakanof* quickly converged to a 2-planet solution that describes our measurements much better than the single planet fit ($\sigma = 0.82 \text{ m s}^{-1}$, $\bar{\chi}^2 = 2.57$ per degree of freedom – Fig. 4). The orbital parameters of the 4.69-day planet change little from the 1-planet fit, except for the eccentricity which increases to $e_2 = 0.20 \pm 0.02$. Its mass is revised down to $M_2 \sin i = 11.09 M_{\oplus}$, and the period hardly changes, $P_2 = 4.6938 \pm 0.0007$ day. The second planet would have a $P_3 = 34.8467 \pm 0.0324$ day period, an $e_3 = 0.20 \pm 0.05$ eccentricity and a minimum mass of $m_3 \sin i = 12.58 M_{\oplus}$. Such periods would correspond to semi-major axes of 0.04 and 0.15 AU. Those are sufficiently disjoint

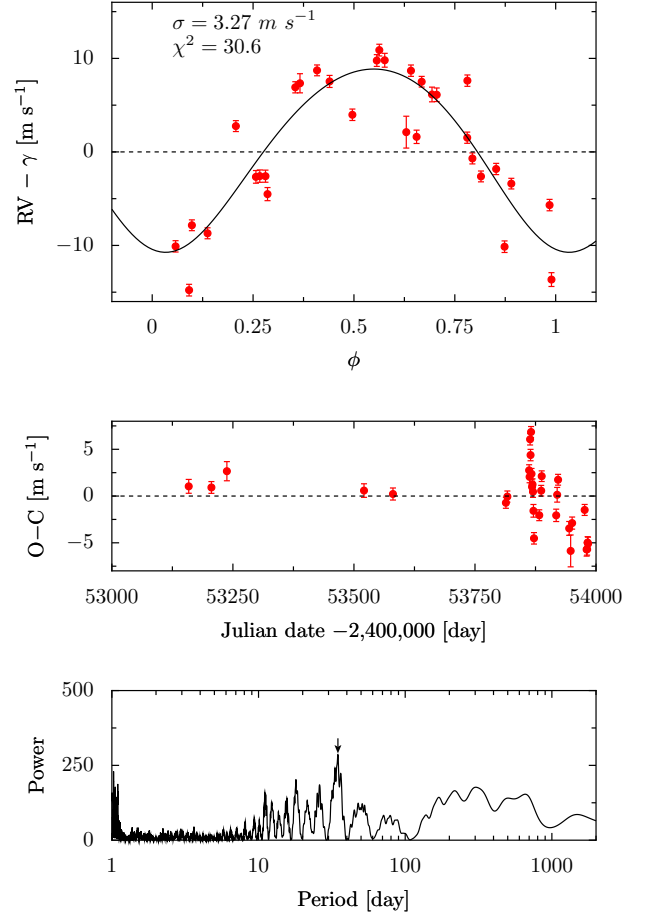


Fig. 3. *Upper panel:* Radial velocities of GJ 674 (red filled circles) phase-folded to the 4.6940 days period of the best 1-planet fit (curve). The dispersion around the fit ($\sigma = 3.27 \text{ m s}^{-1}$) and its reduced chi-square ($\bar{\chi}^2 = 30.6$ per degree of freedom) indicate that a single planet does not describe the data very well. *Middle panel:* Radial-velocity residuals of the 1-planet fit *Bottom panel:* The Lomb-Scargle periodogram of the residuals shows a broad peak centered around 35 days.

that mutual interactions can be neglected over observable time scales, and that the system would be stable over longer time scales.

The low dispersion around the solution and the lack of any significant peak in the Lomb-Scargle periodogram of its residuals shows that our current radial-velocity measurements contain no evidence for an additional component.

5. Activity analysis

Apparent Doppler shifts unfortunately do not always originate in the gravitational pull of a companion: in a rotating star, stellar surface inhomogeneities such as plages and spots can break the exact balance between light emitted in the red-shifted and blue-shifted halves of the star. Observationally, these inhomogeneities translate into flux variations as well as into changes of both the shape and the centroid of spectral lines (Saar & Donahue 1997; Queloz et al. 2001). Spots typically also impact spectral indices, whether designed to probe the chromosphere (to which photospheric spots have strong magnetic connections), or the photosphere (because spots have cooler spectra). Of the two candidate periods, the 4.69-day one is unlikely to reflect stellar rotation. We measure from our GJ 674 spectra a rotational velocity of $v \sin i \lesssim 1 \text{ km s}^{-1}$, which would need a rather improbable stellar

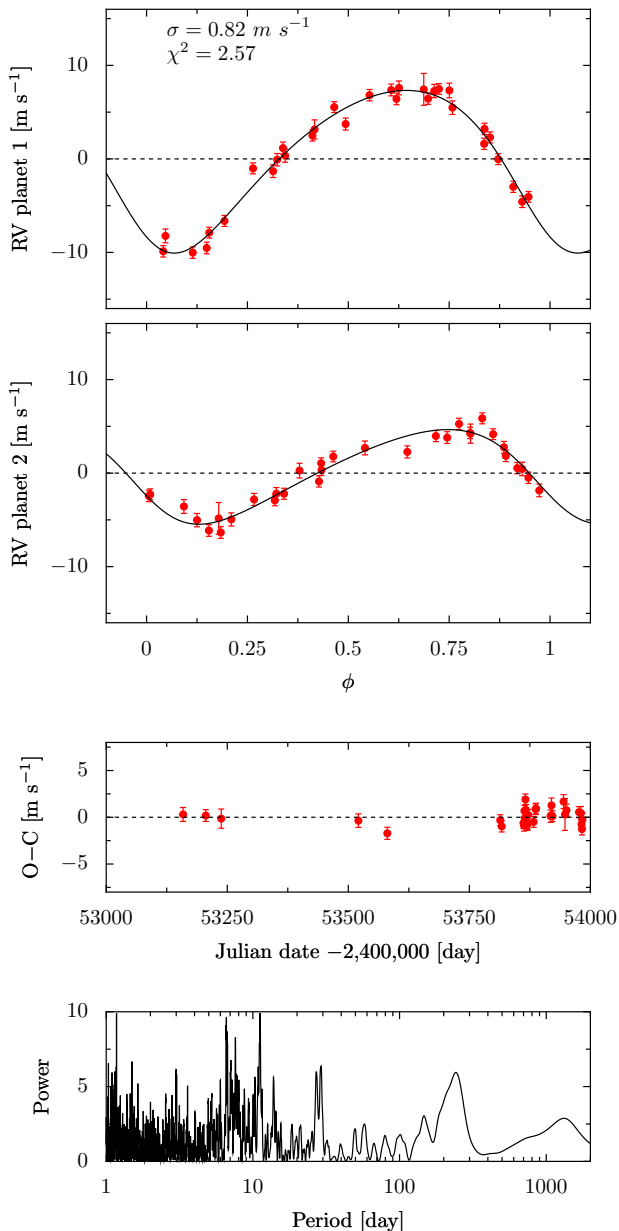


Fig. 4. *Top two panels:* Radial velocity measurements phased to each of the two periods, after subtraction of the other component of our best 2-planet Keplerian model. *Third panel:* Residuals of the best 2-planet fit as a function of time (O–C, Observed minus Computed). *Bottom panel:* Lomb-Scargle periodogram of these residuals.

inclination ($i \lesssim 15^\circ$) to match such a short period. The moderate activity level of GJ 674 on the other hand leaves the nature of the second signal a priori uncertain, and the very small rotation velocity removes much of the power of the usual bisector test (Appendix A). We therefore investigated its magnetic activity through photometric observations (§5.1) and detailed examination of the chromospheric features in the clean HARPS spectra (§5.2).

5.1. Photometric variability

We obtained photometric measurements with the CCD camera of the Euler Telescope (La Silla) during 21 nights between September 2nd and October 19th 2006. GJ 674 was observed through a VG filter which, amongst the available filters, opti-

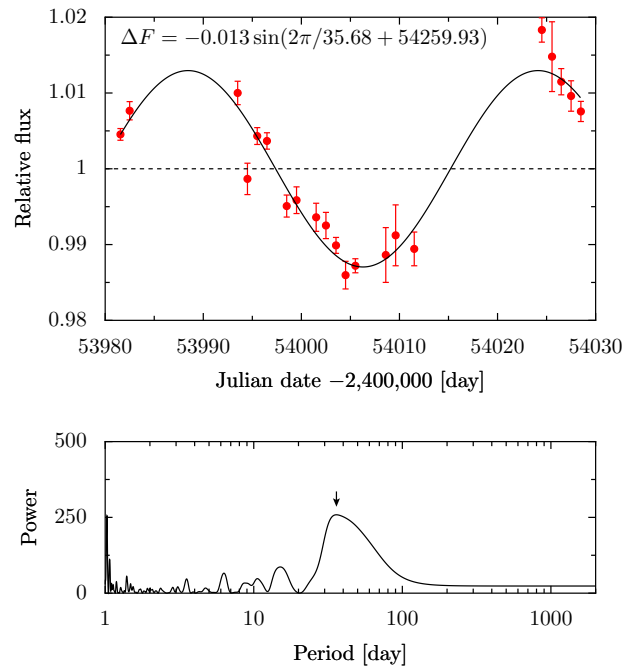


Fig. 5. *Upper panel:* Differential photometry of GJ 674 as a function of time. The star clearly varies with a 1.3% amplitude. *Bottom panel:* The periodogram of the GJ 674 photometry exhibits significant power excess peaked at 35 days (small black arrow).

mizes the flux ratio between GJ 674 and its two brightest reference stars. This relatively blue filters also happens to have good sensitivity to spots on cool stars such as GJ 674. To minimize atmospheric scintillation noise we took advantage of the low stellar density to defocus the images to $\text{FWHM} \sim 11''$, so that we could use longer exposure times. The increased read-out and sky background noises from the larger synthetic aperture which we then had to use remain negligible compared to both stellar photon noise and scintillation.

We gathered 14 to 75 images per night with a median exposure time of 20 seconds. We used the Sept. 24th data, which have the longest nightly time base, to tune the parameters of the IRAF DAOPHOT package and optimize the set of reference stars (HD 157931, CD 4611534 and 7 anonymous fainter stars) to minimize the dispersion in the GJ 674 photometry for that night. These parameters were then fixed for the analysis of the full data set. The nightly light curves for GJ 674 were normalized by that of the sum of the references, clipped at 3σ to remove a small number of outliers, and averaged to one measurement per night to examine the long term photometric variability of GJ 674. GJ 674 clearly varies with a $\sim 1.3\%$ amplitude, and a (quasi-)period close to 35 days (Fig. 5). To verify that this variability does not actually originate in one of the reference stars, we repeated the analysis alternately using as reference star HD 157931 alone and the average of the 8 other references. Both light curves are very similar to Fig. 5.

The photometric observations are consistent with the signal of a single spot, within the limitations of their incomplete phase coverage: the variations are approximately sinusoidal, and their ~ 0.2 - 0.3 radian phase shift from the corresponding radial velocity signal closely matches the difference expected for a spot. The spot would cover 2.6% of the stellar surface if completely dark, corresponding to a $\sim 0.16 R_{\star}$ radius for a circular spot.

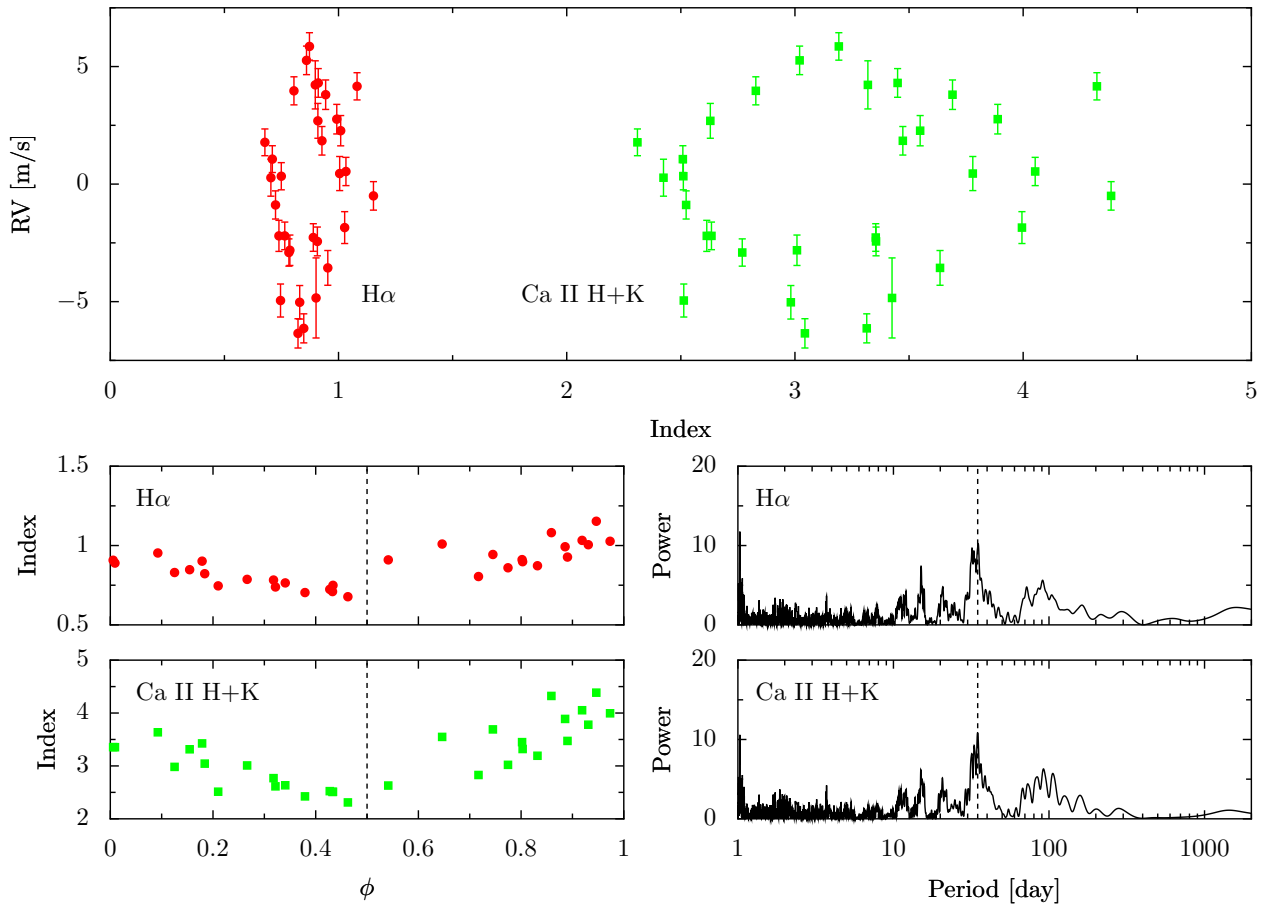


Fig. 6. *Upper panel:* Differential radial velocity of GJ 674, corrected for the signature of the 4.69 days planet in our 2-planet Keplerian fit, as a function of the $H\alpha$ (red filled circles) and $Ca\ II\ H\&K$ (green filled squares) spectral indices defined in the text. *Bottom right panels:* the $Ca\ II\ H\&K$ and $H\alpha$ indexes phased to the longer period of the 2-planet Keplerian model. *Bottom left panels:* Power Density spectra of the spectroscopic indexes. A clear power excess peaks at 34.8 days (vertical dashed lines).

5.2. Variability of the spectroscopic indices

The emission reversal in the core of the $Ca\ II\ H\&K$ resonant lines results from non-radiative heating of the chromosphere, which is closely coupled to spots and plages through magnetic connections between the photosphere and chromosphere. The $H\alpha$ line is similarly sensitive to chromospheric activity. We measured these chromospheric spectral features results in the clean HARPS spectra used to measure the radial velocities, and examine their variability.

Like the well known Mt. Wilson S index (Baliunas et al. 1995), our $Ca\ II\ H\&K$ index is defined as:

$$\text{Index} = \frac{H + K}{B + V}. \quad (1)$$

with H and K sampling the two lines of the $Ca\ II$ doublet, and B and V the continuum on both sides of the doublet. Our H and K intervals are 31 km s^{-1} wide and centered on 3933.664 and 3968.47 \AA , while B and V are respectively integrated over $[3952.6, 3956\text{ \AA}]$ and $[3974.8, 3976\text{ \AA}]$.

This H+K index varies with a clear period of ~ 34.8 days (Fig. 6). Within the combined errors this is consistent with both the photometric period and the longer radial velocity period. The phasing of the chromospheric index and the photometry is such that lower photometric flux matches higher $Ca\ II$ emission, as expected if active chromospheric regions hover over photospheric spots.

A plot of the (apparent) radial-velocity as a function of the H+K spectral index similarly shows the characteristic loop pattern expected for a spot. The radial velocity effect of a spot cancels out when it crosses the sub-observer meridian, which occurs twice during a rotation period: once on the hemisphere facing the observer, and once on the opposite hemisphere. During the front-facing crossing the spot has maximal projected area, hence maximal chromospheric emission, while it has a minimal projected area (and is possibly hidden, depending on its latitude and the stellar inclination) during the back-facing crossing. As a result, both extrema of the chromospheric index correspond to radial-velocity zero-crossings. At intermediate phases the spot produces intermediate chromospheric emission levels, and it induces positive (respectively negative) radial-velocity shifts when the masked area is on the rotationally blue- (respectively red-shifted) half of the star. The net result in a plot of chromospheric emission as a function of radial velocity is a closed loop.

Chromospheric filling-in of photospheric $H\alpha$ absorption has similarly been found a powerful activity diagnostic for M dwarfs. Kürster et al. (2003) found that in Barnard's star it correlates linearly with the radial-velocity variations, and interpreted that finding as evidence that active plage regions inhibit the convective velocity field. The variation pattern in GJ 674 definitely differs from a linear correlation between $H\alpha$ and the radial-velocity residuals, and needs a different explanation.

Similarly to Kürster et al. (2003) we define our $H\alpha$ index as:

$$\text{Index} = \frac{F_{H\alpha}}{F_1 + F_2}. \quad (2)$$

with $F_{H\alpha}$ sampling the $H\alpha$ line, and F_1 and F_2 the continuum on both sides of the line. Our $F_{H\alpha}$ interval is 31 km s^{-1} wide and centered on 6562.808 \AA , while F_1 and F_2 are respectively integrated over $[6545.495, 6556.245 \text{ \AA}]$ and $[6575.934, 6584.684 \text{ \AA}]$. The $H\alpha$ index behaves similarly to the Ca II H+K index.

The chromospheric indices vary by factors of ~ 2 and ~ 1.3 (for our specific choices of continuum windows), and are thus much more contrasted than the photometry. They do not however vary as smoothly with phase as the photometry, perhaps due to (micro-)flares. This somewhat reduces their value as diagnostics of spot-induced radial velocity variations, but these measurements on the other hand require no new observation. They undoubtedly reinforce the spot interpretation here, and they will be extremely useful in cases where photometry cannot be immediately obtained.

5.3. Planets vs. activity

In §4 we showed that our 32 radial-velocity measurements of GJ 674 are well described by two Keplerian signals, as illustrated by the low reduced chi-square of that model. The above analysis (§5) however demonstrates that the rotation period of GJ 674 coincides with the longer of the two Keplerian periods. Both the stellar flux and the Ca II H+K emission vary with that period, implying that the surface of GJ 674 has a magnetic spot. This spot must induce radial-velocity changes, with the observed phase relative to the photometric signal. As a consequence, some, and probably all, of the 35-day radial-velocity signal must originate in the spot. Planet-induced activity through magnetic coupling (e.g. Shkolnik et al. 2005) would in principle be an alternative explanation of the correlation, but here it is not a very attractive one: the inner planet is at least as massive as the hypothetical 35-day planet, and would, at least naively, be expected to have stronger interactions with the magnetosphere of GJ 674. The 4.69-day period however is only seen in the radial velocity signal, and it has no photometric or chromospheric counterpart.

6. Discussion

6.1. Characteristics of GJ 674b

Perhaps the most important result of the above analysis is that the ~ 4.69 -day planet of GJ 674 is robust: variability identifies the stellar rotation period as ~ 35 days, and the 4.69-day period therefore cannot reflect rotation modulation. The short period signal, in spite of its larger amplitude, also has no counterpart in either photometry or chromospheric emission, further excluding a signal caused by magnetic activity.

The 1-planet fit, which effectively treats the activity signal as white noise, results in a minimum mass for GJ 674b of $m_2 \sin i = 12.7 M_{\oplus}$. The 2-planet fit by contrast filters out this signal. That filtering obviously uses a physical model which is not completely appropriate, but that remains preferable to handling a (partly) coherent signal as white noise. We therefore adopt the corresponding estimate of the minimum mass, $m_2 \sin i = 11.09 M_{\oplus}$.

At 0.039 AU from its parent star, the temperature of GJ 674 b is $\sim 450 \text{ K}$. Planets above a few Earth masses planets can, but

need not, accrete a large gas fraction, leaving its composition – mostly gaseous or mostly rocky – unclear. The orbital eccentricity might shed light on the structure of GJ 674b, if confirmed by additional measurements: rocky and gaseous planets have rather different dissipation properties, and significant eccentricity at the short period of GJ 674 b needs a high Q factor, unless it is pumped by an additional planet at a longer period (e.g. Adams & Laughlin 2006). For now, the stellar activity leaves the statistical significance of the eccentricity slightly uncertain, and we therefore prefer to stay clear from overinterpreting it.

6.2. Properties of M-dwarf planets

One important motivation in searching for planets around M dwarfs is to investigate whether the planet-metallicity correlation found for Jupiter-mass planets around solar-type stars extends to very-low-mass stars. Our photometric calibration of M dwarfs metallicity (Bonfils et al. 2005b) gives respective metallicities of $[\text{Fe}/\text{H}] = -0.03, -0.25, +0.14, +0.03,$ and -0.28 for GJ 436, GJ 581, GJ 849, GJ 876 and GJ 674. M dwarfs with known planets therefore have an average metallicity of -0.078 and a median of -0.03 . By comparison, the 44 M dwarfs of the Bonfils et al. (2005b) volume limited sample which are not currently known to host a planet have average and median metallicities of -0.181 and -0.160 . M dwarfs with planets therefore appear slightly more metal-rich than M dwarfs without planets. A Kolmogorov-Smirnov test (Press et al. 1992) of the two samples gives an 11% probability that they are drawn from the same distribution. The significance of the discrepancy is therefore still modest, limited by small-number statistics.

One can additionally note that the two stars which host giant planets, GJ 876 and GJ 849, occupy the metal-rich tail of the M dwarf metallicity distribution, with GJ 849 almost as metal-rich as the most metal-rich star of the comparison sample. The next most metal-rich of the M dwarfs with planets, GJ 436, has an additional long-period companion ($P > 6 \text{ yr}$) which might well be a giant planet (Maness et al. 2006) and would then strengthen that trend. If confirmed by additional data, this would validate the theoretical predictions (Ida & Lin 2004; Benz et al. 2006) that only Jovian-mass planets are more likely to form around metal-rich stars. Current observations are consistent with this prediction, but not yet very conclusively so (Udry et al. 2006).

Much recent theoretical work has gone into examining how planet formation depends on stellar mass. Within the “core accretion” paradigm, Laughlin et al. (2004) and Ida & Lin (2005) predict that giant planet formation is inhibited around very-low-mass stars, while Neptune-mass planets should inversely be common. Within the same paradigm, but assuming that M dwarfs have denser protoplanetary disks, Kornet et al. (2006) predict instead that Jupiter-mass planets become more frequent in inverse proportion to the stellar mass. Finally, Boss (2006) examines how planet formation depends on stellar mass for planets formed by disk instability, and concludes that frequency of Jupiter-mass planet is independent of stellar mass, as long as disks are massive enough to become unstable.

To date, none of the ~ 300 M dwarfs scrutinized for planets by the various radial-velocity searches (Bonfils et al. 2006; Endl et al. 2006; Butler et al. 2006) has been found to host a hot Jupiter. Conversely, GJ 674b is already the 4th hot Neptune. Though that cannot be established quantitatively yet, these surveys are likely to be almost complete for hot Jupiters, which are easily detected. Hot Neptune detection, on the other hand, is definitely highly incomplete. Setting aside this incompleteness for now, simple binomial statistics shows that the probability of

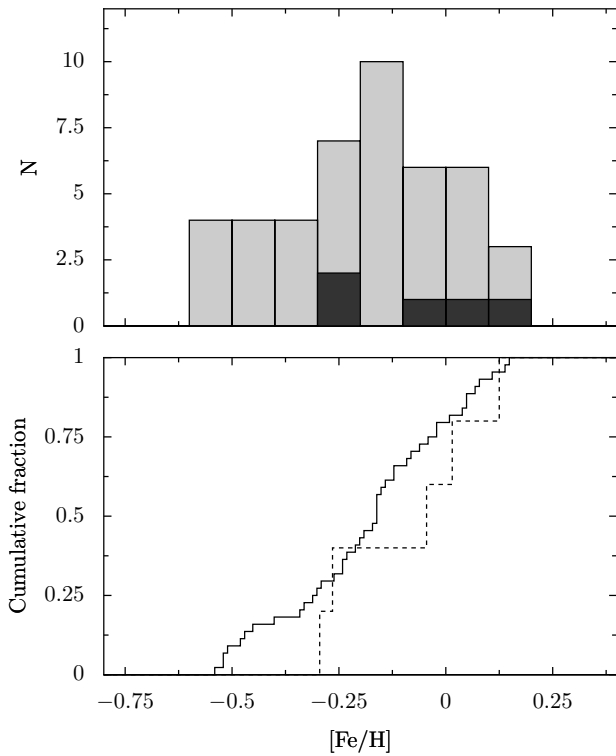


Fig. 7. *Upper panel:* Metallicity distributions of 44 M dwarfs without known planets (gray shading) and of the 5 M dwarfs known to host planets (black shading). *Bottom panel:* Corresponding cumulative distributions (solid and dashed lines, respectively).

Table 2. Keplerian parameterization for GJ 674b and GJ 674's spot.

Parameter		GJ 674b	Spot
P	[days]	4.6938 ± 0.007	34.8467 ± 0.0324
T	[JD]	2453780.085 ± 0.078	2453767.13 ± 0.92
e		0.20 ± 0.02	0.20 ± 0.05
ω	[deg]	143 ± 6	113 ± 9
K	[m s^{-1}]	8.70 ± 0.19	5.06 ± 0.19
$a_1 \sin i$	[AU]	$3.68 \cdot 10^{-6}$	$1.59 \cdot 10^{-5}$
$f(m)$	[M_{\odot}]	$3.0 \cdot 10^{-13}$	$4.4 \cdot 10^{-13}$
$m_2 \sin i$	[M_{Earth}]	11.09	12.58
a	[AU]	0.039	0.147

finding no and 4 detections in 300 draws of the same function is only 3%. There is a thus 97% probability that hot Neptunes are more frequent than hot Jupiter around M dwarfs. Accounting for this detection bias in more realistic simulations (Bonfils et al. in prep.) obviously increases the significance of the difference. Planet statistics around M dwarfs therefore favor the theoretical models which, at short periods, predict more Neptune-mass planets than Jupiter-mass planets.

Acknowledgements. We are grateful to the anonymous referee for constructive comments. XB and NCS acknowledge support from the Fundação para a Ciência e a Tecnologia (Portugal) in the form of fellowships (references SFRH/BPD/21710/2005 and SFRH/BPD/8116/2002) and a grant (reference POCI/CTE-AST/56453/2004). The photometric monitoring has been performed on the EULER 1.2 meter telescope at La Silla Observatory. We are grateful to the SNF (Switzerland) for its continuous support. This research has made use of the SIMBAD database, operated at CDS, Strasbourg, France.

References

Adams, F. C. & Laughlin, G. 2006, *ApJ*, 649, 1004
 Baliunas, S. L., Donahue, R. A., Soon, W. H., et al. 1995, *ApJ*, 438, 269

Beaulieu, J.-P., Bennett, D. P., Fouqué, P., et al. 2006, *Nature*, 439, 437
 Benz, W., Mordasini, C., Alibert, Y., & Naef, D. 2006, in *Tenth Anniversary of 51 Peg-b: Status of and prospects for hot Jupiter studies*, ed. L. Arnold, F. Bouchy, & C. Moutou, 24–34
 Bond, I. A., Udalski, A., Jaroszyński, M., et al. 2004, *ApJ*, 606, L155
 Bonfils, X., Delfosse, X., Udry, S., Forveille, T., & Naef, D. 2006, in *Tenth Anniversary of 51 Peg-b: Status of and prospects for hot Jupiter studies*, ed. L. Arnold, F. Bouchy, & C. Moutou, 111–118
 Bonfils, X., Delfosse, X., Udry, S., et al. 2005a, *A&A*, 442, 635
 Bonfils, X., Forveille, T., Delfosse, X., et al. 2005b, *A&A*, 443, L15
 Boss, A. P. 2006, *ApJ*, 643, 501
 Bouchy, F., Pepe, F., & Queloz, D. 2001, *A&A*, 374, 733
 Butler, R. P., Johnson, J. A., Marcy, G. W., et al. 2006, *ArXiv Astrophysics e-prints*
 Butler, R. P., Vogt, S. S., Marcy, G. W., et al. 2004, *ApJ*, 617, 580
 Cutri, R. M., Skrutskie, M. F., van Dyk, S., et al. 2003, *2MASS All Sky Catalog of point sources. (The IRSA 2MASS All-Sky Point Source Catalog, NASA/IPAC Infrared Science Archive. <http://irsa.ipac.caltech.edu/applications/Gator/>)*
 Delfosse, X., Forveille, T., Mayor, M., et al. 1998, *A&A*, 338, L67
 Delfosse, X., Forveille, T., Ségransan, D., et al. 2000, *A&A*, 364, 217
 Endl, M., Cochran, W. D., Kürster, M., et al. 2006, *ApJ*, 649, 436
 ESA. 1997, *VizieR Online Data Catalog*, 1239, 0
 Gould, A., Udalski, A., An, D., et al. 2006, *ApJ*, 644, L37
 Hawley, S. L., Gizis, J. E., & Reid, N. I. 1997, *AJ*, 113, 1458
 Hünsch, M., Schmitt, J. H. M. M., Sterzik, M. F., & Voges, W. 1999, *Late-type stars in the ROSAT all-sky survey*, ed. B. Aschenbach & M. J. Freyberg, 387–+
 Ida, S. & Lin, D. N. C. 2004, *ApJ*, 604, 388
 Ida, S. & Lin, D. N. C. 2005, *ApJ*, 626, 1045
 Kornet, K., Wolf, S., & Różyńska, M. 2006, *A&A*, 458, 661
 Kürster, M., Endl, M., Rouesnel, F., et al. 2003, *A&A*, 403, 1077
 Laughlin, G., Bodenheimer, P., & Adams, F. C. 2004, *ApJ*, 612, L73
 Leggett, S. K. 1992, *ApJS*, 82, 351
 Leggett, S. K., Allard, F., Geballe, T. R., Hauschildt, P. H., & Schweitzer, A. 2001, *ApJ*, 548, 908
 Lovis, C., Mayor, M., Pepe, F., et al. 2006a, *Nature*, 441, 305
 Lovis, C., Mayor, M., Pepe, F., Queloz, D., & Udry, S. 2006b, in *Precision Spectroscopy in Astrophysics*
 Maness, H. L., Marcy, G. W., Ford, E. B., et al. 2006, *ArXiv Astrophysics e-prints*
 Marcy, G. W., Butler, R. P., Fischer, D., et al. 2001, *ApJ*, 556, 296
 Marcy, G. W., Butler, R. P., Vogt, S. S., Fischer, D., & Lissauer, J. J. 1998, *ApJ*, 505, L147
 Mayor, M., Pepe, F., Queloz, D., et al. 2003, *The Messenger*, 114, 20
 McArthur, B. E., Endl, M., Cochran, W. D., et al. 2004, *ApJ*, 614, L81
 Pepe, F., Mayor, M., Queloz, D., et al. 2004, *A&A*, 423, 385
 Press, W. H., Teukolsky, S. A., Vetterling, W. T., & Flannery, B. P. 1992, *Numerical recipes in C. The art of scientific computing* (Cambridge: University Press, —c1992, 2nd ed.)
 Queloz, D., Henry, G. W., Sivan, J. P., et al. 2001, *A&A*, 379, 279
 Rivera, E. J., Lissauer, J. J., Butler, R. P., et al. 2005, *ApJ*, 634, 625
 Saar, S. H. & Donahue, R. A. 1997, *ApJ*, 485, 319
 Santos, N. C., Bouchy, F., Mayor, M., et al. 2004, *A&A*, 426, L19
 Shkolnik, E., Walker, G. A. H., Bohlender, D. A., Gu, P.-G., & Kürster, M. 2005, *ApJ*, 622, 1075
 Turon, C., Creze, M., Egret, D., et al. 1993, *Bulletin d'Information du Centre de Données Stellaires*, 43, 5
 Udalski, A., Jaroszyński, M., Paczyński, B., et al. 2005, *ApJ*, 628, L109
 Udry, S., Mayor, M., Benz, W., et al. 2006, *A&A*, 447, 361

Appendix A: Bisector analysis

As demonstrated by Saar & Donahue (1997) the bisector analysis loses much of its diagnostic power when applied to slow rotators. In simulations of the impact of star spots on radial-velocity and bisector measurements, they found that, for a given spot configuration, the radial velocity varies linearly with $v \sin i$ while the bisector span varies as $(v \sin i)^{3.3}$. The bisector signal therefore decreases faster with decreasing rotational velocities than the radial-velocity signal, and disappears faster in measurement noise. For GJ 674 we measure a very low rotation velocity ($v \sin i < 1 \text{ km s}^{-1}$). It is therefore unsurprising that the cor-

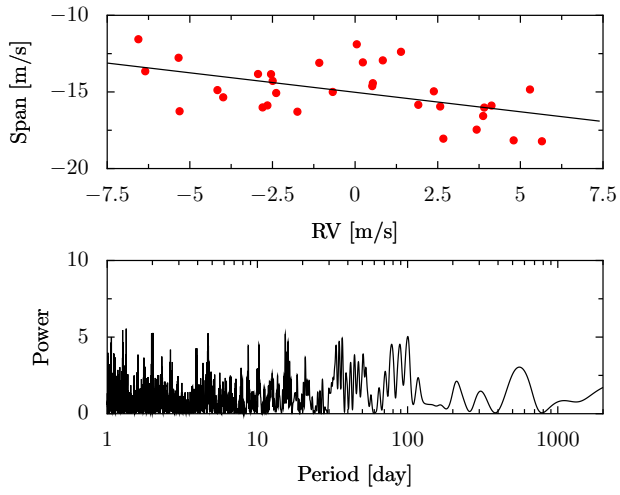


Fig. A.1. Bisector analysis for GJ 674 measurements

relation between the bisector span and radial velocity is weak (Fig. A.1) and not statistically significant.